Spatiotemporal alterations of autophagy marker LC3 in rat skin fibroblasts during wound healing process

Fukushima J. Med. Sci.,
Vol. 64, No. 1, 2018

[Original Article]

Spatiotemporal alterations of autophagy marker LC3 in rat skin fibroblasts during wound healing process

Emiko Asai[1)], Masaya Yamamoto[2)#], Kazuki Ueda[1)] and Satoshi Waguri[2)]

[1)]Department of Plastic and Reconstructive Surgery, Fukushima Medical University, 1-Hikarigaoka, Fukushima City, Fukushima, Japan, [2)]Department of Anatomy and Histology, Fukushima Medical University, 1-Hikarigaoka, Fukushima City, Fukushima, Japan

(Received October 27, 2016, accepted December 6, 2017)

Abstract

To investigate the possible implications of autophagy, one of the degradation pathways induced by metabolic stress, in the dynamic reconstructive process of wound healing, the appearance and changes of punctate structures for microtubule-associated protein 1 light chain 3 (LC3), an autophagosome marker, were examined in a rat skin wound healing model. Although the ratio of LC3-II/LC3-I in Western blotting was not evidently changed during the wound healing process, LC3-positive dots were clearly observed in fibroblasts and myofibroblasts, and occasionally in macrophages, by immunohistofluorescence microscopy. Some of the LC3-positive dots were colocalized with Atg16L signal, an isolation membrane marker, and electron microscopy revealed the presence of typical autophagosomes in fibroblasts near the margin of the wound. The number of LC3-positive dots per fibroblast increased during the later period of the proliferation phase, and interestingly, it was higher in the margin than the center of the wound. It was also high in the periwound skin area. These results suggest that drastic functional changes in fibroblasts during wound healing process are accompanied by the alteration of the autophagy-lysosomal degradation system.

Key words : autophagosome, Atg16L, immunohistofluorescence

Introduction

The process of skin wound healing, including regenerative and reconstructive processes at both tissue and cellular levels, is extremely dynamic[1)]. After wounding, the inflammatory phase firstly begins with cytokines and growth factors, such as Transforming growth factor (TGF) β1/2/3, Platelet derived growth factor (PDGF), Fibroblast growth factor (FGF)1/2/4/7/10, Epidermal growth factor (EGF), and Vascular endothelial growth factor (VEGF), playing a role in attracting macrophages and lymphocytes for sweeping degenerative tissue and for exerting defense mechanisms. The secondary phase of the proliferation follows, which is characterized by a buildup of granulation tissues with angiogenesis to fill up the defective space. Fibroblast activities of migration, proliferation, and type III collagen synthesis are known to be regulated by several factors during this phase. Thirdly, in the remodeling phase, type III collagen is replaced by type I collagen, and fibroblasts are differentiated into myofibroblasts that play a role in wound contraction and scar maturation. Even after the completion of epithelial resurfacing, scar remodeling continues for an additional 1-2 years in human. It has been known that pathological alteration in these complicated processes may cause chronic wound and pathological scar formation.

The autophagy-lysosome pathway is one of the intracellular degradation systems that is induced under metabolic stress such as amino acid starvation.

[#]Present address : Department of Health Science, Uekusa Gakuen University, 1639-3 Ogura-cho Wakaba-ku, Chiba-City, Chiba, Japan
Corresponding author : Satoshi Waguri E-mail : waguri@fmu.ac.jp
https://www.jstage.jst.go.jp/browse/fms http://www.fmu.ac.jp/home/lib/F-igaku/

The process of autophagy involves appearance and dynamic changes of membranous organelles. Upon autophagy signal, a portion of the cytoplasm, which often contains organelles, is segregated by a double-membrane structure, called the isolation membrane or phagophore. When the isolation membrane is closed, it becomes an autophagosome, which then fuses with the lysosome forming autolysosome, in which segregated materials together with the inner membrane are degraded for reuse. To date, over 30 autophagy-related (Atg) genes have been identified. Among the core Atg proteins, the Atg12-5-16L complex is known as a marker of the isolation membrane because it is localized on this membrane during its growth and is detached shortly after the closing process[2]. Also, microtubule-associated protein 1 light chain 3 (LC3) is a mammalian homologue of Atg8 and is a well-known autophagosome marker. It can exist in cells as two forms, LC3-I and LC3-II. Upon autophagy signal, a cytosolic-type LC3-I can be conjugated with phosphatidylethanolamine by the actions of ubiquitin-like conjugation systems involving Atg7, Atg3, Atg10, and Atg12-5-16L, to become LC3-II that is recruited on the isolation membrane. In the autophagosome, LC3-II molecules on the inner membrane are degraded by lysosomal enzymes, while those on the outer membrane are shed by Atg4[3-5]. Therefore, the amounts of LC3-II in Western blotting and the number of LC3-positive dots under an immunohistofluorescence microscopy have been considered as good indicators for estimating the amounts of autophagosomes.

Recently, it became evident that dysfunction of autophagy is associated with pathogenesis of many diseases including neurodegeneration[6-8], cancer[9,10], metabolic disorders[11-13], and microbial infection and inflammatory disorders[10,14-16]. However, in the research field of skin wound healing, there is a report only on autophagy involved in the healing process after burn wounding[17]. We therefore investigated the possible implications of autophagy in a well-established rat wound healing model.

Materials and Methods

Animal model and sampling

Seven-week-old Wistar rats were used in this study. Twenty one rats were used for analyses of Western blot and immnohistofluorescence microscopy (3 rats for each time point as described below), and 2 rats for electron microscopy. The rats were anesthetized by intraperitoneal injection of pentobarbital sodium (somnopentyl®, Kyoritsu Seiyaku Corporation, Tokyo, Japan ; 0.1 mg/100 g body weight). For making a wound, three circular full-thickness skin regions on the back that included the panniculus carnosus were excised with a 10-mm biopsy punch (Kai medical, Tokyo, Japan). Six hours, and 2, 5, 7, 9 and 14 days after operation, one of the wounds along with the surrounding skin regions (approximately 2 mm from the margin) was excised under anesthesia. After removing the epithelial layer, the excised regions were frozen by liquid nitrogen and stored for Western blotting. The rats were further fixed by cardiac perfusion with 4% paraformaldehyde in 0.1 M phosphate buffer (PB, pH 7.4) containing 4% sucrose, and other two wounds together with the surrounding region were excised and processed for immunohistofluorescence microscopy. The specimens were immersed in the same fixative at 4°C for more than one night, followed by standard paraffin- or cryo-embedding procedures as previously described[18]. These animal experiments were approved by Fukushima Medical University Laboratory Animal Research Committee and were compliant with the institution's guidelines and the Japanese Government Animal Protection and Management Law.

Western blot analysis

Frozen specimens were homogenized in lysis buffer (0.1 M Tris-HCl, pH 7.6) including, 150 mM NaCl, 5% glycerol, 1% Triton X-100, 5 mM Ethylenediaminetetraacetic acid (EDTA), protease inhibitor (complete EDTA free Protease inhibitor cocktail tablets ; Roche Diagnostics, Basel, Switzerland), and phosphatase inhibitor (Phosphatase inhibitor Cocktail 2/3, SIGMA-ALDRICH, St. Louis, USA). After centrifugation at 3,000 rpm (800 g) at 4°C for 10 minutes, the supernatant containing 8 μg of protein was separated by Sodium dodecyl sulfate-Polyacrylamide gel electrophoresis (SDS-PAGE) with 4-20% gradient gel and transferred onto mixed ester nitrocellulose membranes (Hybound-C Extra, GE Healthcare Life Sciences, Chicago, USA). Immunoreactions were performed with one of following primary antibodies : Anti-CD68 antibody (ED1) (1 : 1,000, AbD Serotec MCA341R, Kidlington, UK), phosphorylated mitogen-activated protein kinase (pMAPK) (1 : 500, Cell Signaling, Danverse, USA), Prolyl-4-Hydroxylase (1 : 1,000, Acris Antibodies AF5110-1, Herford, Germany), α smooth muscle actin (αSMA) (1 : 1,000, Vector Laboratories VP-S281, Peterborough, UK), Glyceraldehyde 3-phosphate

dehydrogenase (GAPDH) (1 : 1,000, Santa Cruz Biotechnology sc-32233, Santa Cruz, USA), and LC3A (1 : 200, EP1983Y, Epitomics, Burlingame, USA). After incubation with the corresponding secondary antibody, protein-antibody complexes were detected by chemiluminescent reaction using a solution kit (SuperSignal, Thermo Scientific, Waltham, USA) and a detector ImageQuant LAS4000 mini (GE Healthcare Life Sciences, Chicago, USA). Quantification of band signal intensity was performed using a software, ImageJ. Ratio to the value of GAPDH was calculated, which are then normalized to the value of control. For LC3, ratio of LC3-II to LC3-I was calculated.

Immunohistofluorescence microscopy and quantification of LC3-positive dots

Paraffin sections of 5-μm thickness were prepared and deparaffinized, or cryosections of 10-μm thickness were prepared. These sections were immersed in 0.1 M phosphate buffered saline (pH 7.4) containing 0.1% TritonX-100 for washing and permeabilization, and were blocked with 5% normal goat serum. They were then incubated with one or two (for double staining) of the following primary antibodies at 4°C overnight : Anti-LC3 (1 : 200, EP1983Y, Epitomics), LC3 (1 : 500, PM046, MBL, Woods Hole, USA), Prolyl-4-Hydroxylase (1 : 1,000, Acris Antibodies AF5110-1), ED1 (1 : 50, Serotec MCA341R), αSMA (1 : 100, Vector Laboratories VP-S281) and Atg16L (1 : 500, IF12, MBL). The sections were further incubated with one or two of the appropriate secondary antibodies (1 : 500) conjugated with Alexa Fluor 488 or Alexa Fluor 594. Hoechst33342 (1 : 10,000) was used for nuclear staining. After mounting with a medium (Fluoromount : Diagnostic Bio Systems, Pleasanton, USA), sections were observed with a confocal laser microscope (FV1000 ; Olympus, Tokyo, Japan), equipped with a PlanApo N 60× (NA 1.42 oil) lens. For the image acquisition, 5 to 6 of serial optical slices (1-μm thickness for each) were projected into one image using the operating software, FV10-ASW (Olympus, Tokyo, Japan).

For quantification of LC3-positive dots, images of three square regions of 212 × 212 μm in size were randomly acquired from each of the 3 regions of the wound center, wound margin and periwound skin. For each image the number of LC3-positive dots was divided by the number of nuclei, and this ratio was plotted. Statistical analyses were performed by Student's-*t* test or Tukey-Kramer method. A value of $p<0.01$ was considered as significant.

Electron microscopy

Five days after operation, the rats were fixed by perfusion with 0.1 M PB (pH 7.4) containing 2% glutaraldehyde and 2% paraformaldehyde. Wound regions were excised and cut into slices of 0.2-0.5 mm thickness, which were further fixed in the same solution at 4°C for more than one night. They were washed 3 times by 0.1 M PB with 7.5% sucrose and were post-fixed in 7.5% sucrose (0.1 M PB) with 1% OsO_4 at 4°C for 2 hours. Conventional dehydration and embedding procedures were performed as reported previously[18]. Ultra-thin sections of 60-nm thickness were stained by uranyl acetate and lead citrate, and observed with a transmission electron microscope (JEM-1200EX ; JEOL, Tokyo, Japan).

Results

Characterization of rat wound healing model

The wound healing model used in this study was firstly characterized by Hematoxylin-Eosin staining. The standard wound healing steps proceeded in this model were as follows (Fig. 1A). After surgery, inflammatory cells infiltrated into the wounded region during a few days. The skin defect began to be filled up by granulation tissue from day 2. Contraction of the wound tissue proceeded during days 5-9, which was completed by day 14. To confirm the wound healing process, Western blot analyses were performed using some cellular markers (Fig. 1B and C). The signal intensitiy for macrophage marker ED1 increased during days 2-5 and then gradually decreased. Phosphorylated MAP kinase, a cell proliferation marker, increased during days 2-9. P4H, a fibroblast marker, increased from 6 h to days 2-7, while αSMA, a myofibroblast marker, increased after day 5. These results suggest that the inflammatory phase occurs with a peak during days 2-5, the proliferation phase proceeds during the period of days 2-9, and the remodeling phase follows for the days 5-14 in our experimental model. Importantly, these phases largely overlapped each other, suggesting that different phases proceed in parallel within the whole wound tissue.

Biochemical and morphological detections of LC3-II in the wound healing tissues

LC3-II/LC3-I ratio has been used as a biochemical indicator of autophagosome formation[19]. However, Western blot analysis revealed that there was

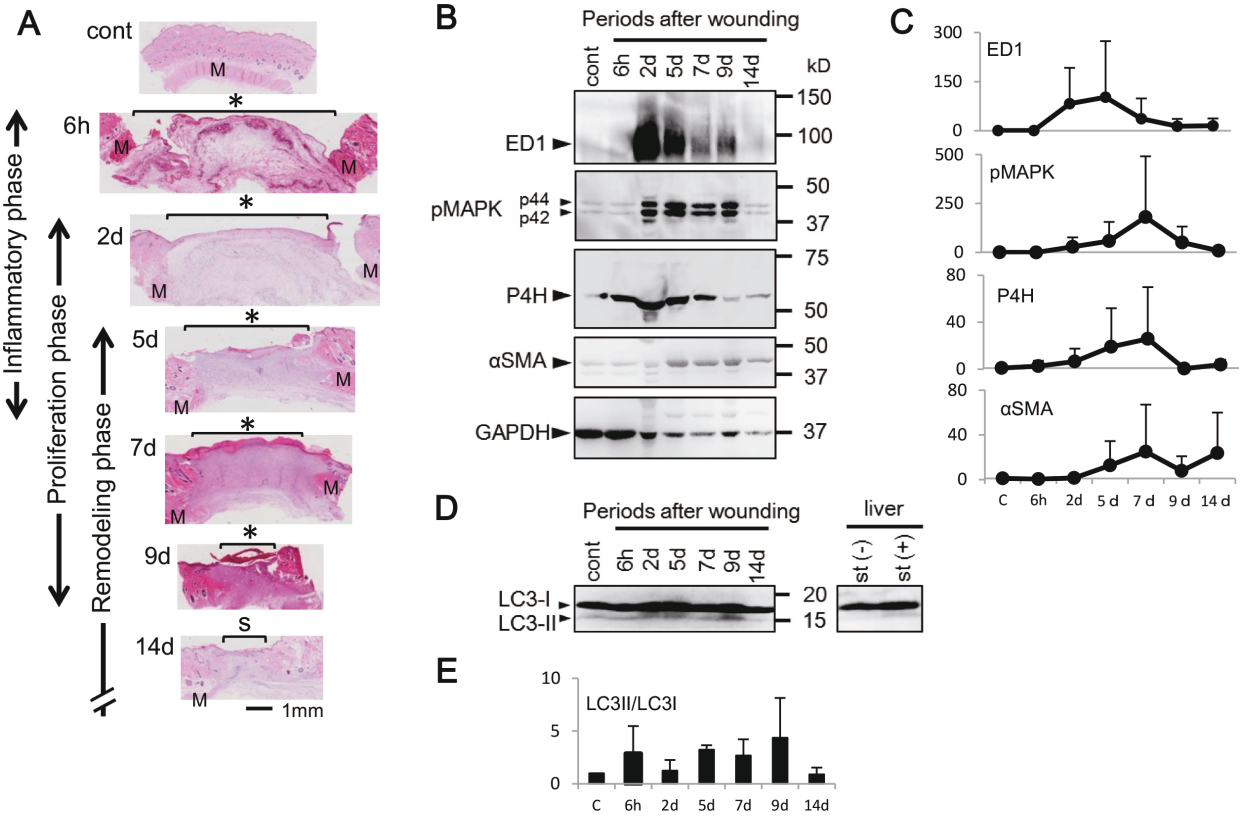

Fig. 1. Rat wound healing model and change of LC3-II expression
Rat control skin (cont) and wounded skin at 6 hour (6 h) and days (d) 2, 5, 7, 9, and 14 after surgery were processed into paraffin sections for Hematoxylin and Eosin (HE) staining (A), or for Western blotting to examine expressions of the following marker proteins : the ED1, pMAPK (p42 and p44), P4H, αSMA, and GAPDH for (B), and LC3 for (D). Rat liver lysates with (st +) or without (st −) 24-hour starvation are shown with positional indicators of LC3-I and LC3-II (D). The intensities of ED1, pMAPK (p42 and p44), P4H and αSMA were normalized with GAPDH and further plotted as the ratio to the control value (C). Ratio of LC3-II to LC3-I (LC3-II/I) was calculated and plotted as the ratio to the control value (E). kD : molecular weight.

no significant alteration during the wound healing process (Fig 1D and E). Because it may have been difficult to detect the differences in homogenized tissues, immunohistofluorescence microscopy was performed to examine the localization of LC3, an autophagosome marker. Formalin-fixed cryosections were double stained with anti-LC3 and one of following antibodies ; P4H, αSMA, and ED1, markers for fibroblasts, myofibroblasts, and activated macrophages, respectively (Fig. 2). In the granulation tissues, punctate signals for LC3 were often observed in P4H-positive fibroblasts and αSMA-positive myofibroblasts (Fig. 2A and B). They were also occasionally observed in ED1-positive macrophages (Fig. 2C). Importantly, a population of LC3-positive dots appeared as a cup shape and/or contained a marker of autophagic isolation membrane, Atg16L (Fig. 2D). Moreover, electron microscopy showed the presence of typical autophagosomes in fibroblasts near the margin of the granulation tissues (Fig. 2E and F). These results suggest that the formation of autophagosomes might be related to fibroblast functions.

Spatiotemporal alterations in LC3-positive dots in wound healing tissue

During the course of observation of LC3 distribution, we noticed that fibroblasts in the margin of wound tissues contained more LC3-positive dots than those in the center (Fig. 3C and D). Therefore, the number of LC3-positive dots per fibroblast was quantified in the wound center, wound margin, and periwound regions (Fig. 3A) during the wound healing process. As shown in Fig. 3E, the number of LC3-positive dots in the wound margin drastically increased at days 7-9 with a peak at day 7 ($p<0.05$, Tukey-Kramer test), while in the center it showed a bimodal fluctuation with a minor peak at day 2, a trough during days 5-7, and a major peak at day 9 ($p<0.05$, Tukey-Kramer test). Among the three regions, the number of LC3-positive dots in the margin was significantly higher than that in the cen-

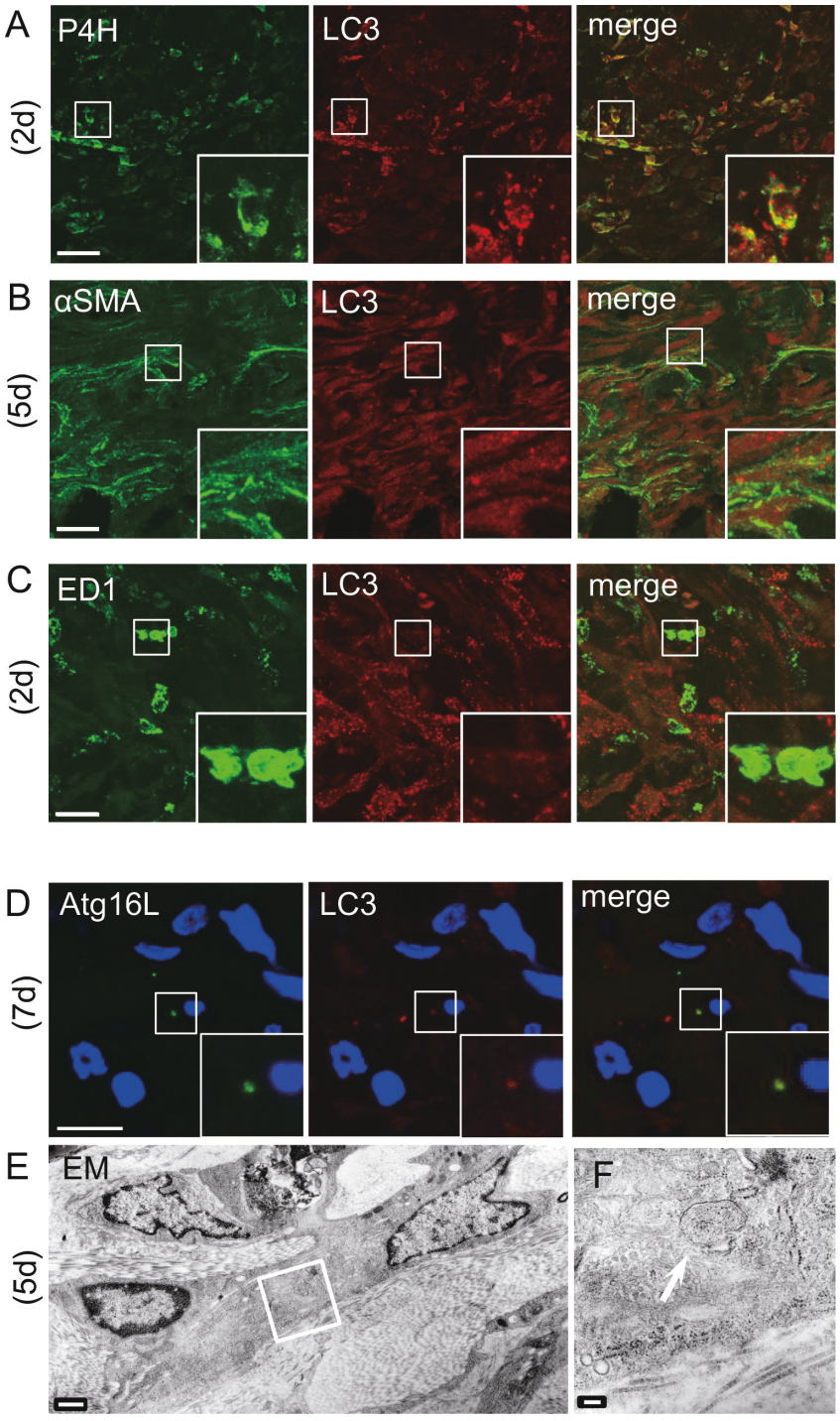

Fig. 2. Histological analyses of LC3-positive cells

(A-C) Wound skin tissues at days 2 and 5 after surgery were fixed and processed for cryosections, which were then double-stained with combinations of following antibodies ; LC3 and P4H (A, green), αSMA (B, green), or ED1 (C, green). Merged images are shown on the right. Boxed regions are magnified in the insets. Bars : 10 μm. (D) Wound skin tissues at day 7 were fixed and processed for paraffin sections, which were double-stained with anti-LC3 (red) and anti-Atg16L (green) antibodies. Merged image containing nuclear staining with Hoechst 33342 (blue) is shown on the right. Bar : 5 μm. (E, F) Wound skin tissues at day 5 were fixed for electron microscopy. The region of wound margin was observed. Boxed region in E is magnified in F. Note that one of the fibroblasts surrounded by collagen fibrils contains a typical autophagosome (arrow in F). Bars : 1 μm in E, 200 nm in F

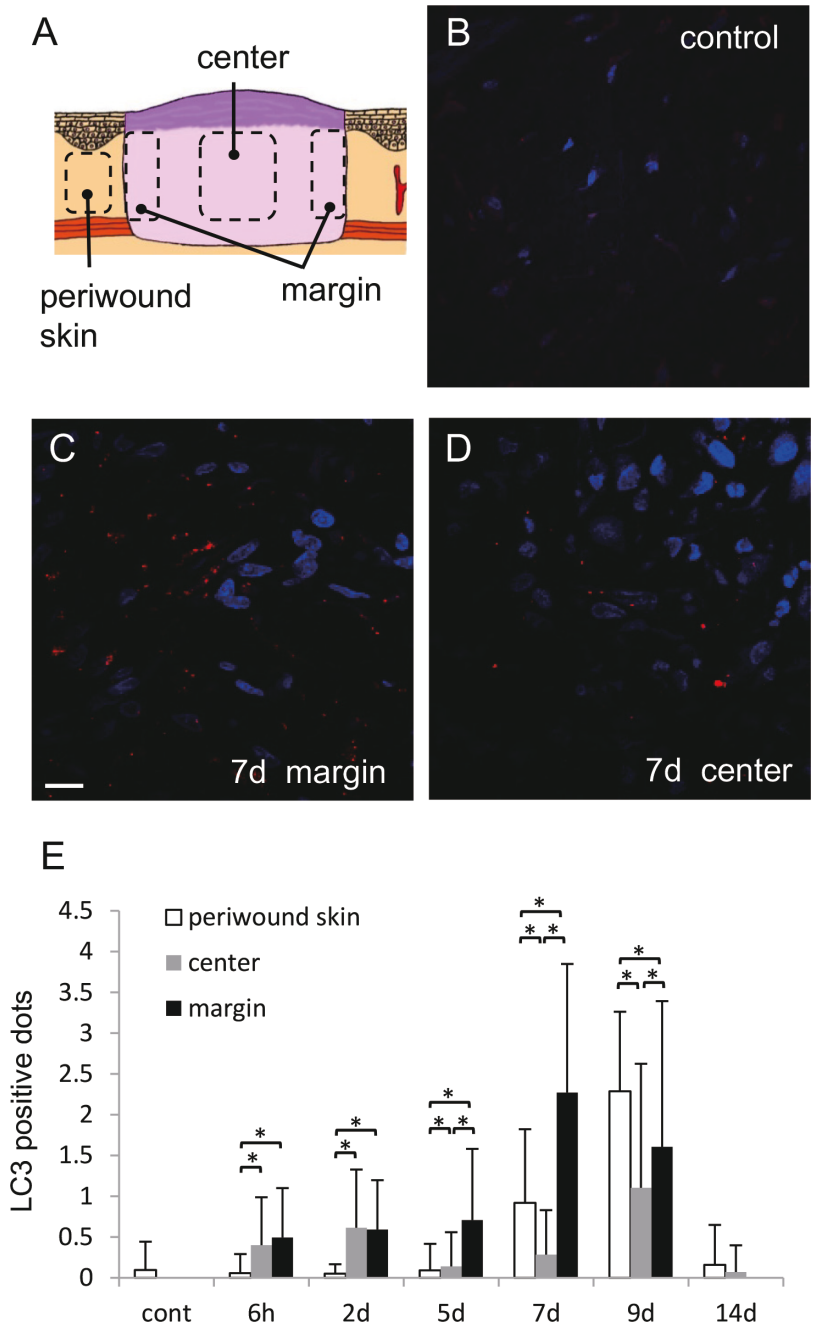

Fig. 3. Spatiotemporal alterations of the LC3-positive dots during the wound healing process
(A) The schematic diagram indicates areas of the periwound skin, center and margin regions of the wound examined in the present study. (B-E) Non-operated control rat skin (B) and wound skin tissues at 6 hours, and days 2, 5, 7, 9, and 14 after surgery were fixed and processed for paraffin sections, which were then stained with anti-LC3 antibody and Hoechst 33342. Margin (C) and center (D) regions of the wound tissues at day 7 are shown. Bar : 10 μm. Ratio of the number of LC3-positive dots to the number of nuclei was calculated (mean±SD) for each region over the time course as described in the materials and methods and plotted in (E). The number of dots at day 14 (#) was counted for the whole wound region, because the margin and center regions could not be discriminated. The differences between the 3 regions were analyzed in (E) (* : $p<0.05$, ANOVA, Tukey-Kramer test for 6 h, 2, 5, 7, and 9 d, and Student's *t* test for 14 d).

ter at days 5, 7, and 9 (Fig. 3 E ; $p<0.05$, Tukey-Kramer test), with magnitudes of 5-, 8-, and 1.5-times, respectively. The regions of periwound skin as well as the skin from rats without the operation was also analysed as a control, where fibroblasts contained only background levels of LC3-postive dots until day 5 (Fig. 3B and E). Unexpectedly, however, the number of LC3-positive dots in this

region drastically increased at days 7–9 ($p<0.05$), being higher than that in the margin or center region ($p<0.05$). The number of LC3-positive dots in the three regions decreased to background levels at day 14.

Discussion

In this study, we examined the number of LC3-positive dots in fibroblasts by immunohistofluorescence microscopy during the course of skin wound healing, and found as follows : (1) The number of LC3-positive dots was increased during days 7 to 9 after the skin wounding, the period which corresponded to the late phase of proliferation or middle phase of remodeling[1]. (2) The number of LC3-positive dots was higher in the margin than the center of the wound, and was also increased in the periwound skin during days 7 to 9. These results suggest that autophagy is related to the function of fibroblasts in the skin wound healing process. How do such spatiotemporal fluctuations of LC3-positive dots reflect fibroblast functions in wound healing? Fibroblasts migrate into the wound region where functional conversions should occur from a phase of migration to that of collagen synthesis and proliferation. After filling-up the defected region, these fibroblasts further differentiate into myofibroblasts contributing to wound contraction[20]. As for the fibroblast migration, Tuloup-Minguez *et al.* reported that suppression of autophagy in mouse embryonic fibroblasts (MEF) or HeLa cells enhanced migration property, which was mediated by promoting the membrane recycling of β1 integrin[21]. In our results, the numbers of LC3-positive dots in both margin and center of the wound were slightly higher than those in the periwound region at day 2. Although it would be difficult to judge the phase of fibroblasts in the margin, our data may support the notion that autophagy is relevant in the ceasing of fibroblast migration. Interestingly, we found that LC3-positive dots remarkably increased in the wound margin during the late phase of proliferation. Because we used skin-defect model, the sequential change of fibroblasts in the wound margin should precede the events that would occur in the center region. Actually, the number of LC3-positive dots in the margin peaked at day 7, then those in the center became highest at day 9 (Fig. 3D). Moreover, we recently observed numerous αSMA-positive myofibroblasts in the margin at day 7 (unpublished data). From the aspect of cell proliferation, most growth signals activate the mechanistic target of rapamycin (mTOR), which usually causes autophagy suppression[22]. In fact, it has recently been reported that bFGF signaling axis activates mTOR, and suppresses autophagy activity in MEFs[23]. This mechanism may support the lower signal for LC3 in the center region than the margin. Thus, it is most likely that the fibroblasts in the margin are under a differentiation phase, suggesting that autophagy functions in relation to the differentiation of fibroblasts into myofibroblasts during wound healing. In this study, we surprisingly found that LC3-positive dots increased in the periwound skin during the latter period of the proliferation phase. It would be difficult to imagine the cellular activities of migration, collagen production, proliferation, and differentiation, because no apparent change was observed in this region in the HE staining. Probably, growth factors and cytokines produced in the wound region and/or a tension caused by wound contraction might be involved.

Recently, Xiao *et al.* reported that activation of autophagy by the treatment of rapamycin suppressed burn wound progression in a rat model of a deep second-degree burn[17]. It has been also reported that enhanced autophagy by rapamycin reduces the infarction size in myocardial ischemia model[24]. Although these studies demonstrated autophagy activation using some biochemical markers, they did not consider other well-known effects of rapamycin. This agent is also known to suppress immunoreaction, cell proliferation, and protein synthesis, through inhibition of mTOR[25]. In fact, production of some collagen molecules is reportedly suppressed by rapamycin treatment. Therefore, effects of rapamycin may be complicated in the full thickness skin wound model, which should be tested in the future.

In conclusion, this study uncovered the involvement of autophagy-lysosomal system in the functional changes of fibroblasts during the wound-healing process. Unfortunately, this study could not elucidate how autophagy-lysosomal system is affected in these experiments, for example whether increase in LC3-positive dots in fibroblasts are caused by autophagy induction or lysosomal suppression. Although further intensive studies are required, we believe that these findings would shed light on future studies on mechanisms for the formation of chronic wound and pathological scar.

Acknowledgments

We thank Atsuko Yabashi for her technical help

in the morphological experiments and the members of the Department of Anatomy and Histology and Department of Plastic and Reconstructive Surgery for their helpful comments in discussions. This work was supported by JSPS KAKENHI Grant Numbers 15H04670

Conflict of Interest Disclosure

There are no conflicts of interest to disclose.

References

1. Gurtner GC, Werner S, Barrandon Y, Longaker MT. Wound repair and regeneration. Nature, **453** : 314–321, 2008.
2. Mizushima N, Komatsu M. Autophagy : renovation of cells and tissues. Cell, **147** : 728–741, 2011.
3. Kabeya Y, Mizushima N, Ueno T, *et al.* LC3, a mammalian homologue of yeast Apg8p, is localized in autophagosome membranes after processing. EMBO J, **19** : 5720–5728, 2000.
4. Kabeya Y, Mizushima N, Yamamoto A, Oshitani-Okamoto S, Ohsumi Y, Yoshimori T. LC3, GABARAP and GATE16 localize to autophagosomal membrane depending on form-II formation. J Cell Sci, **117** : 2805–2812, 2004.
5. Shpilka T, Weidberg H, Pietrokovski S, Elazar Z. Atg8 : an autophagy-related ubiquitin-like protein family. Genome Biol, **12** : 226, 2011.
6. Hara T, Nakamura K, Matsui M, *et al.* Suppression of basal autophagy in neural cells causes neurodegenerative disease in mice. Nature, **441** : 885–889, 2006.
7. Komatsu M, Waguri S, Chiba T, *et al.* Loss of autophagy in the central nervous system causes neurodegeneration in mice. Nature, **441** : 880–884, 2006.
8. Komatsu M, Wang QJ, Holstein GR, *et al.* Essential role for autophagy protein Atg7 in the maintenance of axonal homeostasis and the prevention of axonal degeneration. Proc Natl Acad Sci U S A, **104** : 14489–14494, 2007.
9. Mathew R, Karantza-Wadsworth V, White E. Role of autophagy in cancer. Nat Rev Cancer, **7** : 961–967, 2007.
10. Levine B, Kroemer G. Autophagy in the pathogenesis of disease. Cell, **132** : 27–42, 2008.
11. Ebato C, Uchida T, Arakawa M, *et al.* Autophagy is important in islet homeostasis and compensatory increase of beta cell mass in response to high-fat diet. Cell Metab, **8** : 325–332, 2008.
12. Singh R, Kaushik S, Wang Y, *et al.* Autophagy regulates lipid metabolism. Nature, **458** : 1131–1135, 2009.
13. Yang L, Li P, Fu S, Calay ES, Hotamisligil GS. Defective hepatic autophagy in obesity promotes ER stress and causes insulin resistance. Cell Metab, **11** : 467–478, 2010.
14. Levine B, Deretic V. Unveiling the roles of autophagy in innate and adaptive immunity. Nat Rev Immunol, **7** : 767–777, 2007.
15. Schmid D, Munz C. Innate and adaptive immunity through autophagy. Immunity, **27** : 11–21, 2007.
16. Levine B, Mizushima N, Virgin HW. Autophagy in immunity and inflammation. Nature, **469** : 323–335, 2011.
17. Xiao M, Li L, Hu Q, *et al.* Rapamycin reduces burn wound progression by enhancing autophagy in deep second-degree burn in rats. Wound Repair Regen, **21** : 852–859, 2013.
18. Waguri S, Komatsu M. Biochemical and morphological detection of inclusion bodies in autophagy-deficient mice. Methods Enzymol, **453** : 181–196, 2009.
19. Mizushima N, Yoshimori T. How to interpret LC3 immunoblotting. Autophagy, **3** : 542–545, 2007.
20. Darby IA, Laverdet B, Bonte F, Desmouliere A. Fibroblasts and myofibroblasts in wound healing. Clin Cosmet Investig Dermatol, **7** : 301–311, 2014.
21. Tuloup-Minguez V, Hamai A, Greffard A, Nicolas V, Codogno P, Botti J. Autophagy modulates cell migration and beta1 integrin membrane recycling. Cell Cycle, **12** : 3317–3328, 2013.
22. Jung CH, Ro SH, Cao J, Otto NM, Kim DH. mTOR regulation of autophagy. FEBS Lett, **584** : 1287–1295, 2010.
23. Lin X, Zhang Y, Liu L, *et al.* FRS2alpha is essential for the fibroblast growth factor to regulate the mTOR pathway and autophagy in mouse embryonic fibroblasts. Int J Biol Sci, **7** : 1114–1121, 2011.
24. McCormick J, Suleman N, Scarabelli TM, Knight RA, Latchman DS, Stephanou A. STAT1 deficiency in the heart protects against myocardial infarction by enhancing autophagy. J Cell Mol Med, **16** : 386–393, 2012.
25. Huang S, Bjornsti MA, Houghton PJ. Rapamycins : mechanism of action and cellular resistance. Cancer Biol Ther, **2** : 222–232, 2003.